ROYAL SOCIETY OF CHEMISTRY

COMMUNICATION

Check for updates

Unveiling the catalytic potency of a novel hydrazone-linked covalent organic framework for the highly efficient one-pot synthesis of 1,2,4-triazolidine-3-thiones†

Pankaj Teli, Shivani Soni, Sunita Teli and Shikha Agarwal [ID] *

A novel hydrazone-linked covalent organic framework (TRIPOD-DHTH COF) was synthesized through the ultrasonic treatment of 2,5-dihydroxyterephthalohydrazide (DHTH) and 4,4′,4″-[1,3,5-triazine-2,4,6-triyltris(oxy)]tris-benzaldehyde (TRIPOD). The COF was extensively analyzed using FT-IR, PXRD, SEM, TEM, BET, XPS, TGA, and DTA techniques. The characterization studies revealed the presence of mesoporous properties and high thermal stability, with a surface area measuring 2.78 m^2 g^{-1} and an average pore size of 8.88 nm. The developed COF demonstrated exceptional catalytic activity in synthesizing 1,2,4-triazolidine-3-thiones from thiosemicarbazide and various ketones and aldehydes using a water : ethanol (1 : 2) medium at room temperature. A significant yield (80–98%) of 1,2,4-triazolidine-3-thiones was obtained in a low reaction time (4–20 min). The role of TRIPOD as a precursor in the synthesis of the COF and as a reactant in the synthesis of 1,2,4-triazolidine-3-thione (**3l**) was found to be fascinating. The synthesized COF maintained its catalytic activity over eight runs, underscoring its efficiency and reusability, highlighting its potential for sustainable chemical syntheses.

Introduction

Covalent Organic Frameworks (COFs) have emerged as a revolutionary category of crystalline porous polymers, constructed from organic molecules linked by strong covalent bonds.[1] These substances are acclaimed for their structural diversity, high surface area, and tunable porosity, making them highly versatile for various applications.[2] COFs are formed through the reticulation of organic units into ordered two-dimensional (2D) or three-dimensional (3D) frameworks, enabling the design of materials with specific functionalities.[3]

Synthetic Organic Chemistry Laboratory, Department of Chemistry, Mohanlal Sukhadia University, Udaipur, Rajasthan, India. E-mail: shikhaagarwal@mlsu.ac.in; pankajteli802@gmail.com

The synthesis of COFs involves the condensation of organic monomers with complementary functional groups, such as aldehydes, amines, and boronic acids, resulting in a variety of linkage types including imine, boronate ester, and triazine bonds. These linkages contribute to the robustness and stability of the COFs, allowing them to maintain their structure under various conditions.[4,5] COFs have demonstrated tremendous potential in various sectors due to their exceptional properties. They are used in catalysis,[6–9] gas storage and separation,[10,11] sensing,[12,13] drug delivery,[14,15] energy storage,[16] and environmental remediation.[17] Their unique structural properties and functional capabilities continue to drive research and innovation, promising exciting future developments in various scientific and industrial fields.
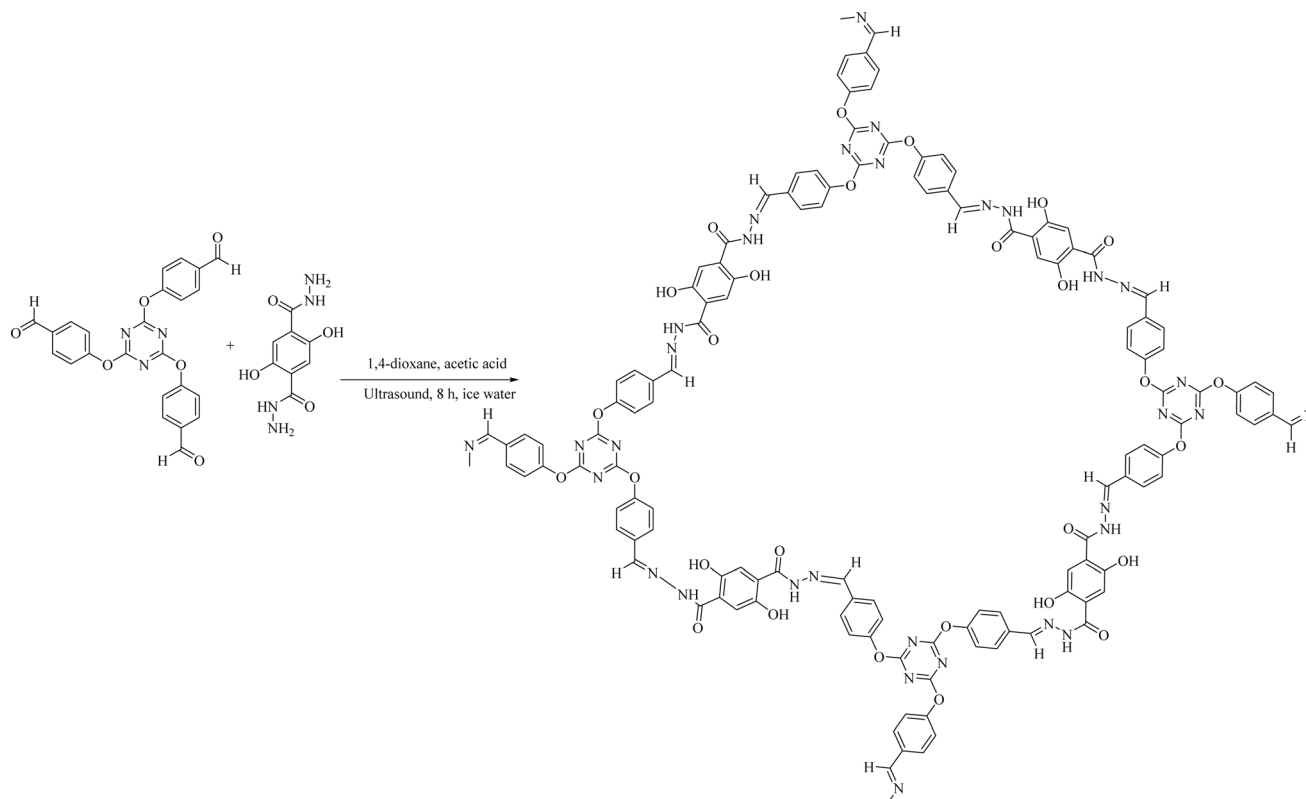
In recent years, the potential of COFs as heterogeneous catalysts in organic transformations has attracted considerable attention.[18,19] Due to their ordered porous structure, they provide a unique environment that allows for the encapsulation of reactants and promotes catalytic activity through enhanced mass transfer and stabilization of reaction intermediates.[20] Several studies have demonstrated the catalytic efficiency of COFs in C–C coupling reactions,[21] cycloadditions, and other organic transformations.[22] The modular nature of COF synthesis allows for the design of materials with specific functional groups or active sites tailored for catalytic applications.[23] However, despite these advances, the COFs in heterocyclic synthesis, particularly for the preparation of biologically active compounds such as triazolidine derivatives, remain underexplored.[24]

Synthesis of heterocyclic moieties is a pivotal aspect of organic chemistry.[25–30] Triazolidines are an important class of heterocyclic compounds, particularly due to their pharmacological relevance. These five-membered heterocycles, containing nitrogen and sulfur atoms, exhibit a wide range of biological activities, including acetylcholinesterase inhibitory activity,[31] and antimicrobial,[32,33] antioxidant,[34] antifungal,[35] antitubercular,[36] and anticancer[37] properties. Their structural versatility and ability to interact with biological targets make them attractive scaffolds in drug discovery. As a result, the development of efficient and
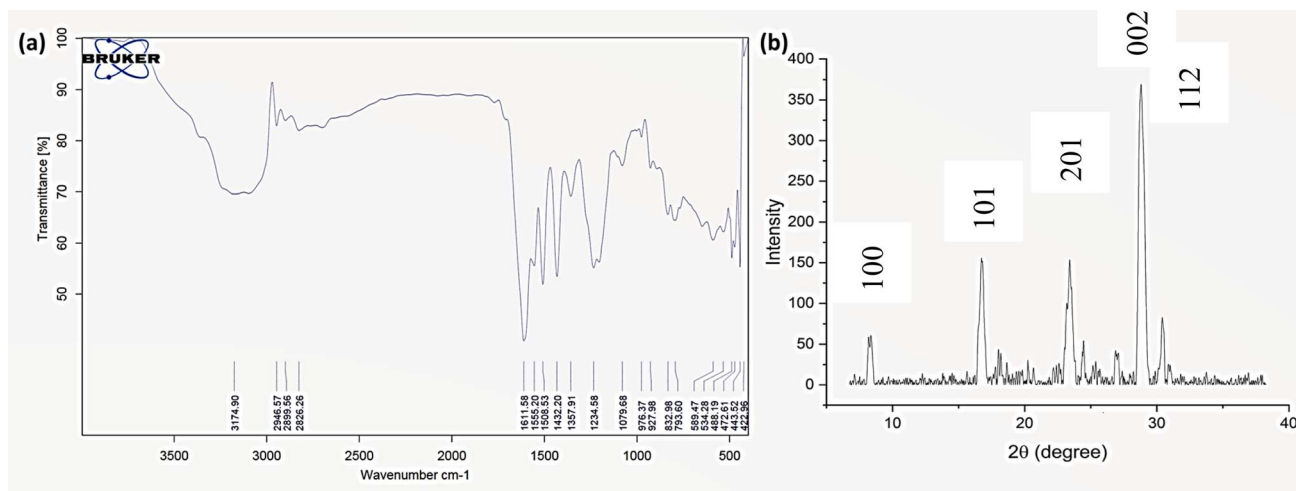
Scheme 1 Preparation of the COF.

Fig. 1 (a) FT-IR spectrum of the synthesized COF; (b) PXRD pattern of the prepared COF.

green methods for the synthesis of triazolidines has become a key area of research in synthetic organic chemistry.

The preparation of triazolidines traditionally involves the condensation of thiosemicarbazides with aldehydes or ketones under acidic or basic conditions. Several classical methods rely on heating the reactants in organic solvents, which often leads to low yields and harsh reaction conditions. Recently, green synthetic approaches have gained attention, emphasizing the need for environmentally friendly solvents, lower temperatures, and the

use of heterogeneous catalysts to promote the reaction. The development of green, efficient, and sustainable methodologies for the synthesis of these heterocycles has been a major focus in organic chemistry. COFs, with their tunable functionalization and porous structure, present an ideal platform for promoting such reactions under mild and environmentally benign conditions. Specifically, hydrazone-linked COFs, due to the presence of reactive C=N bonds, can provide catalytic sites for facilitating

nucleophilic additions and cyclization reactions, making them suitable candidates for the synthesis of triazolidine derivatives.

COFs have emerged as efficient catalysts for such transformations, as their tunable porosity, stability, and surface functionalities make them ideal platforms for facilitating cyclization reactions and enhancing reaction efficiency under mild conditions. In this study, we have explored the green synthesis of 1,2,4-triazolidine-3-thiones using a novel hydrazone-linked COF, offering an eco-friendly and efficient pathway for the preparation of these biologically significant molecules.

In this research, the TRIPOD-DHTH COF was synthesized through the ultrasonic treatment of 2,5-dihydroxyterephthalohydrazide (DHTH) and 4,4′,4″-[1,3,5-triazine-2,4,6-triyltris(oxy)]tris-benzaldehyde (TRIPOD). Furthermore, the catalytic activity of the synthesized novel hydrazone-linked COF was explored for the green synthesis of 1,2,4-triazolidine-3-thiones (T-3-Ts) through the reaction of thiosemicarbazide (TSC) with various aldehydes and ketones. Moreover, the role of TRIPOD as a precursor in the synthesis of COFs and as a reactant in the synthesis of 1,2,4-triazolidine-3-thione (3l) was found to be fascinating.

Experimental

Preparation of TRIPOD

TRIPOD was synthesized by a previously reported method.[38] 4.17 mmol (510 mg) of p-hydroxybenzaldehyde, 1.35 mmol (250 mg) of cyanuric chloride, 4.72 mmol (500 mg) of Na_2CO_3, and p-dioxane (20 mL) were introduced to a flask. Then, the mixture was stirred and maintained at reflux under nitrogen for 18 h. After refluxing, the mixture was subjected to vacuum concentration, and the resulting residue was added to chilled water (10 mL). The precipitate was isolated through filtration, rinsed with 5 mL of cold water, and further dried to yield the pure product (441 mg, 74%).

Synthesis of diethyl-2,5-dihydroxyterephthalate (DHTP)

DHTP was synthesized using previous literature.[39] In a flask, 2,5-dihydroxyterephthalic acid (750 mg, 3.78 mmol) and dry ethanol (30 mL) was added. To this mixture, 3 mL of concentrated H_2SO_4 was introduced dropwise and further refluxed for 18 h until the solid fully dissolved. After cooling to RT, 60 mL of DI was added. The resulting residue was extracted using
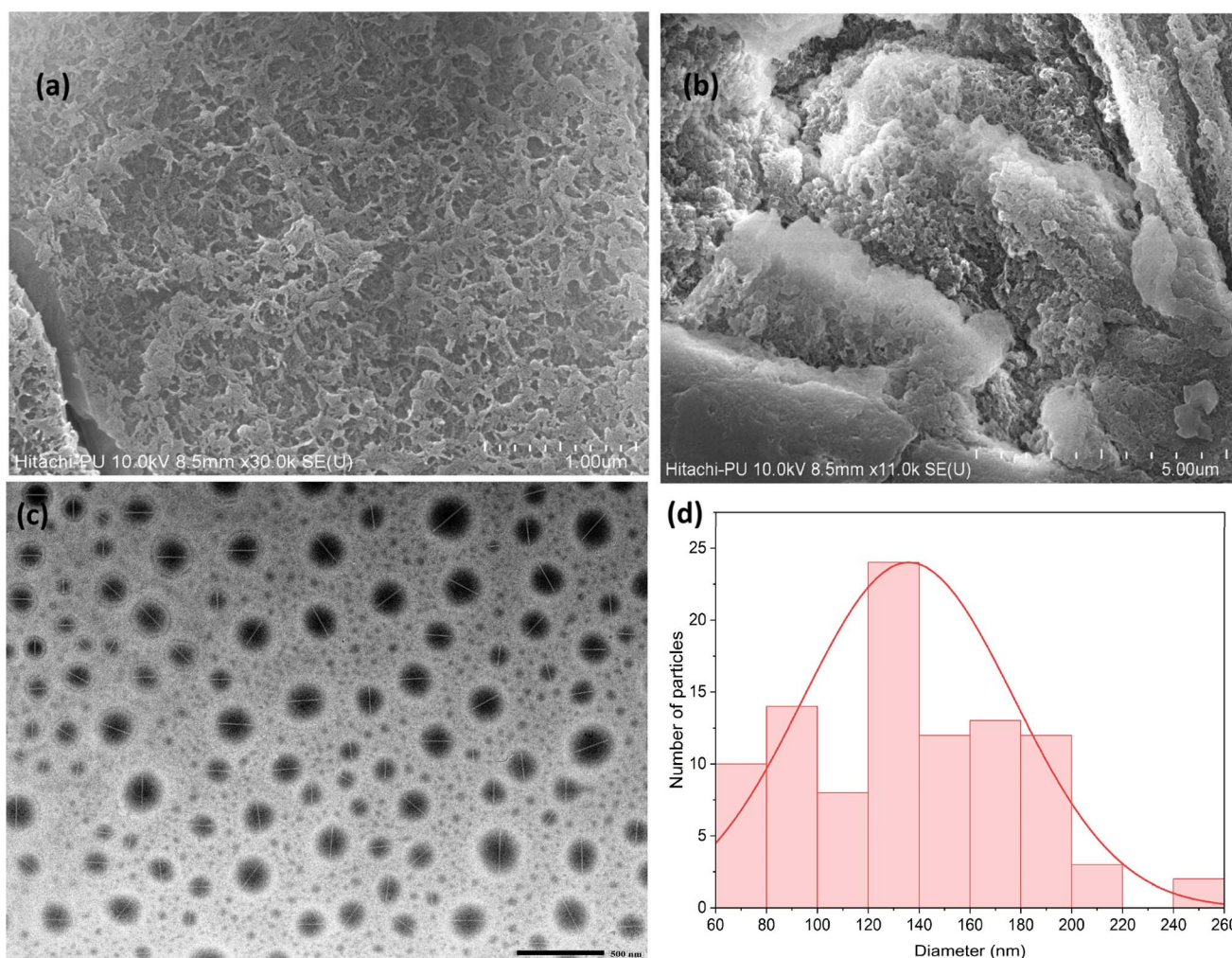

Fig. 2 Surface morphology of the synthesized COF: (a) & (b) the SEM images of the COF; (c) the TEM image of the COF; (d) histogram showing the particle size distribution of the COF.

filtration, thoroughly washed with DI water, and then the compound was subjected to drying in an oven (800 mg, 83.06%).

Synthesis of DHTH

DHTH was synthesized using previous literature.[39] 1.96 mmol (500 mg) of DHTP and ethanol (20 mL) were mixed in a round-bottomed flask (RBF). Then, 51 mmol of hydrazine hydrate (2.5 mL) was introduced to the flask. This solution was heated for 15 h at 90 °C. A pale-yellow precipitate formed after cooling the mixture to RT. The resulting crude product was separated by filtration, rinsed thrice with ethanol, and dried under reduced pressure to obtain the pure compound (330 mg, 74.5%).

Preparation of the TRIPOD-DHTH COF

The method for preparation of a novel COF was adopted from the reported method.[17] A solution of 1,4-dioxane (12 mL) and 6.0 M aqueous acetic acid (2 mL) was added to a beaker containing 0.72 mmol of synthesized DHTH (162 mg) and 0.48 mmol of TRIPOD (112 mg). This mixture was sonicated for 8 hours using an ice water bath. The resulting fluffy yellow solid, which swelled in the solvent system, was isolated through filtration. The formed solid was sequentially rinsed thrice with anhydrous dichloromethane, anhydrous acetone, and tetrahydrofuran, and then activated under vacuum at 120 °C for 8 h to produce the COF (280 mg).

General synthetic approach for triazolidine-3-thione derivatives

In 100 mL RBF, 10 mL of a water : ethanol mixture (1 : 2) was added to a mixture of aldehyde (1.0 mmol), TSC (1.0 mmol), and COF (20 mg) at RT. The progress of the reaction was tracked with TLC. After completion, extra EtOH was used to separate the compound and catalyst. The catalyst was filtered out to achieve separation. The desired compound was obtained by evaporating ethanol under vacuum. The products of the reaction were analyzed and verified with FT-IR, mass, ^{1}H, and ^{13}C NMR spectroscopy.

Results and discussion

We synthesized a novel COF by condensing TRIPOD and DHTH as organic building blocks to create novel hydrazone-linked structures. The synthesis process of COFs was straightforward and involved ultrasonic treatment of a mixture containing the monomers DHTH and TRIPOD in a blend of aqueous CH_3COOH and 1,4-dioxane (Scheme 1). The resulting COF was obtained as a pale-yellow powder, showing insolubility in typical organic solvents, including acetone, alcohols, chloroform, acetonitrile, ethers, dimethyl sulfoxide and N,N-dimethylformamide.

The synthesized COF was subjected to a series of characterization techniques to evaluate its structural, morphological, surface, and thermal properties. The data obtained from FTIR, XRD, SEM, TEM, BET, XPS, TGA, and DTA analyses are discussed below.
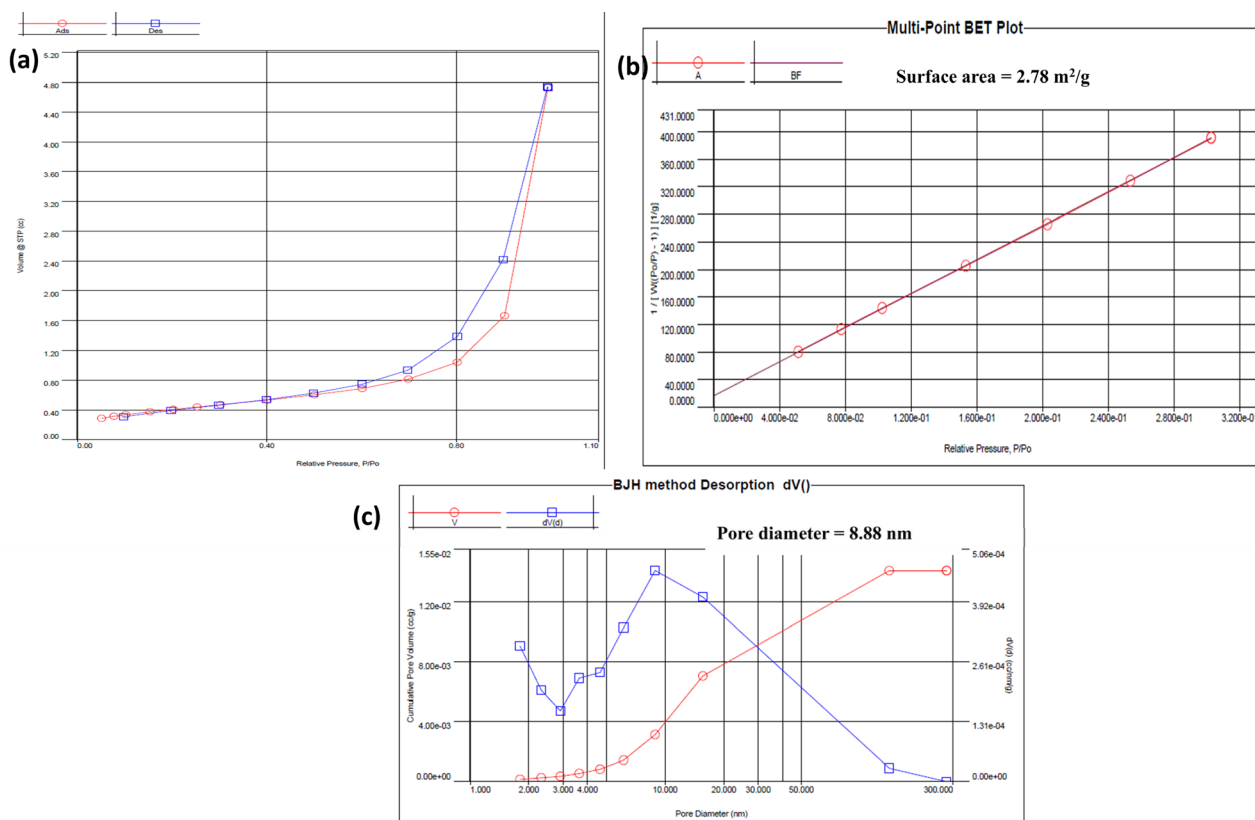

Fig. 3 BET analysis of the COF; (a) N_2 adsorption–desorption isotherms of the COF; (b) BET surface area plot of the COF calculated from the adsorption data; (c) average pore diameter calculation through the BJH desorption method.
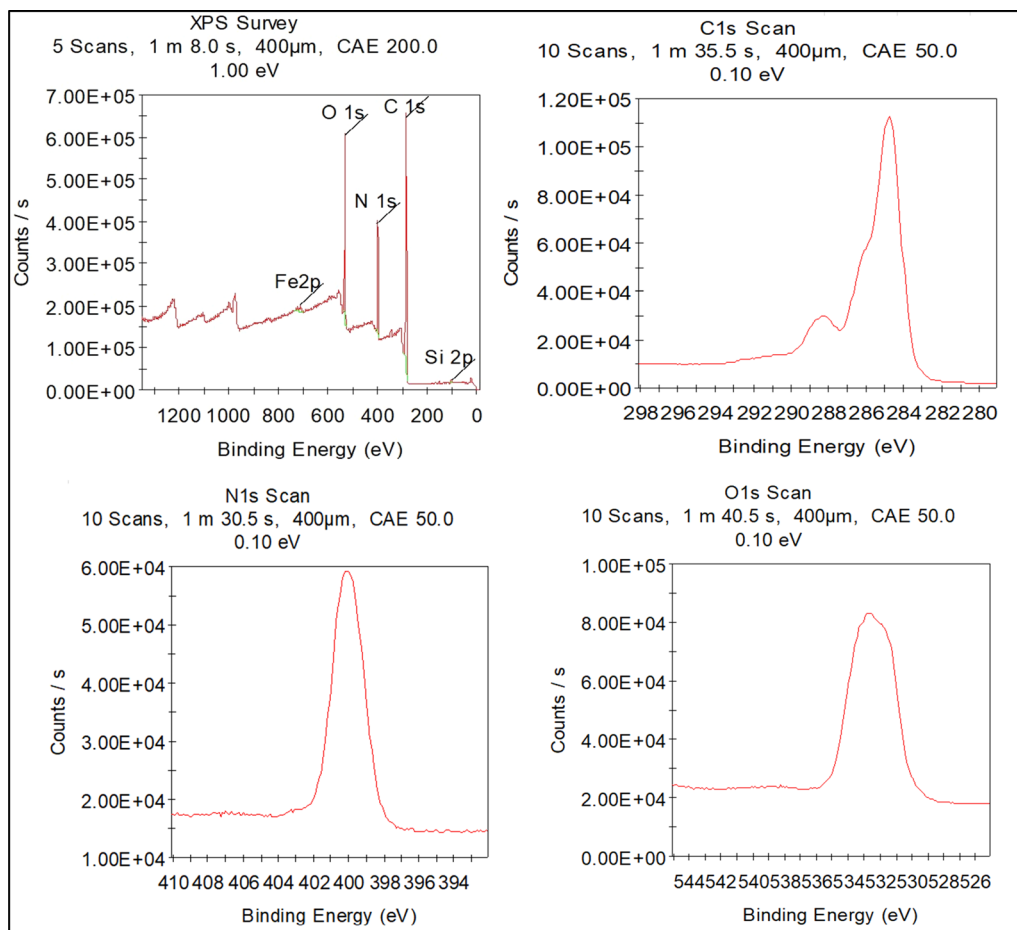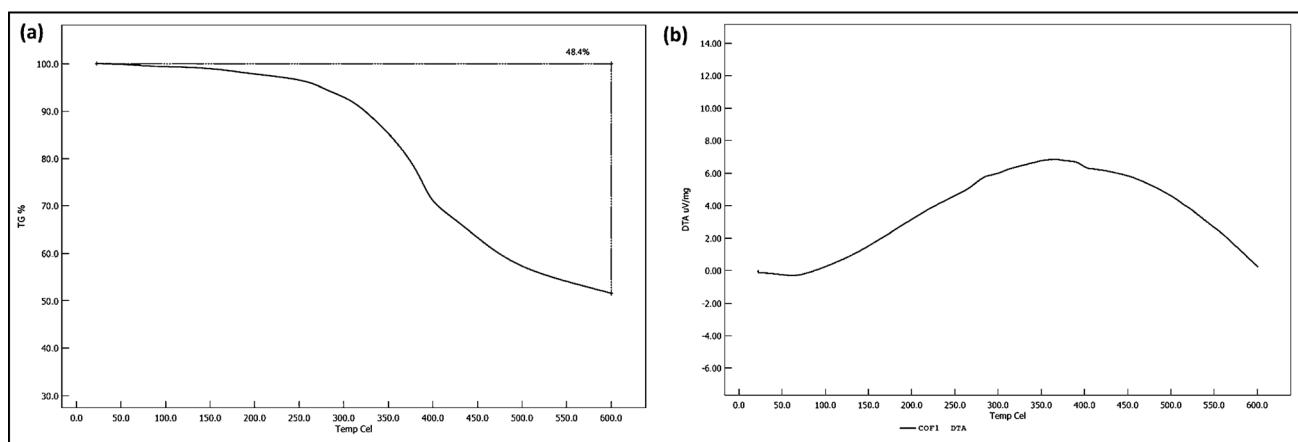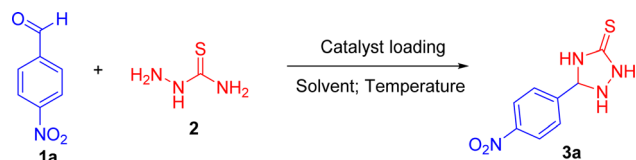
Fig. 4   XPS study of the COF.

Fig. 5   Study about thermal stability of the COF: (a) TGA curve of the COF and (b) DTA curve of the COF.
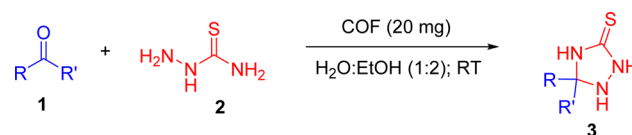
FTIR analysis

Fourier Transform Infrared (FTIR) spectroscopy was employed to confirm the successful formation of the COF and to identify its functional groups. The FTIR spectrum (Fig. 1a) exhibited characteristic absorption bands at 1611 cm^{-1}, corresponding to the C=N stretching vibration in the hydrazone linkage, and at 1234 cm^{-1}, indicative of the C=N stretching in the triazole ring.[40] These peaks confirmed the successful formation of the desired linkages within the COF structure. The absence of significant shifts in these peaks suggests that the COF's framework is chemically stable, a crucial factor for its potential applications in catalysis and adsorption.

Scheme 2 The model reaction involving thiosemicarbazide and 4-nitrobenzaldehyde to optimize conditions.

Scheme 3 General reaction for the preparation of T-3-Ts.

XRD analysis

The crystalline structure of the COF was investigated using Powder X-ray Diffraction (PXRD). The PXRD pattern (Fig. 1b) revealed a sharp, intense peak at 28.88° and several weaker peaks at 8.3°, 16.74°, 18.07°, 23.39°, 24.43°, 26.96°, 30.42°, and 30.95°, indicating a well-ordered crystalline framework.[41] The crystallite size, calculated using the Debye–Scherrer equation, was found to be 23.24 nm. This degree of crystallinity is essential for the COF's functionality, as it impacts the material's stability and its effectiveness in applications requiring a high degree of structural order, such as catalysis.

SEM and TEM analyses

Scanning Electron Microscopy (SEM) and Transmission Electron Microscopy (TEM) were used to analyze the morphology and size distribution of the COF particles. The SEM images (Fig. 2a and b) showed that the COF has a rough surface texture, which is beneficial for adsorption processes, as it increases the available surface area for interactions. The TEM images (Fig. 2c and d) revealed a consistent spherical morphology with an average particle size of approximately 135.90 nm. This uniformity in size and shape indicates that the synthesis process was well-controlled, which is vital for ensuring reproducibility in large-scale applications.

BET surface area and porosity analysis

The surface area and porosity of the COF were characterized using Brunauer–Emmett–Teller (BET) analysis. The nitrogen adsorption–desorption isotherms (Fig. 3) were a type IV isotherm, indicative of a mesoporous structure. The BET surface area was measured to be 2.78 m^2 g^{-1}, and moderate, consistent with the COF's mesoporous nature. The Barrett–Joyner–Halenda (BJH) method was used to calculate an average pore size of 8.88 nm and a total pore volume of 0.014 cm^3 g^{-1}. These characteristics are crucial for catalytic applications, where pore size and surface area directly influence the material's efficiency in facilitating chemical reactions.[42]

XPS analysis

X-ray Photoelectron Spectroscopy (XPS) was utilized to investigate the COF's surface elemental composition and chemical states. The survey XPS spectrum (Fig. 4) detected carbon (C 1s), nitrogen (N 1s), and oxygen (O 1s) as the main elements on the surface. High-resolution C 1s spectra showed peaks at 284.8 eV (C–C/C–H), 286.2 eV (C–N), and 288.5 eV (C=O), confirming the presence of these functional groups. The N 1s peak at 400.2 eV was attributed to sp^2-hybridized nitrogen in triazole rings, assuring the integrity of the COF's nitrogenous components. The O 1s peak at around ~531 eV reflects oxygen atoms, likely originating from hydroxyl or ether groups, enhancing the COF's chemical functionality and adsorption properties. The XPS data suggest that the COF has a surface composition of 64.97% carbon, 14.57% nitrogen, and 19.3% oxygen, consistent with the designed molecular structure.

TGA

Thermogravimetric Analysis (TGA) was conducted to assess the thermal stability of the COF. The TGA curve (Fig. 5a) shows an initial minor weight loss at around 100 °C, attributed to the desorption of adsorbed moisture. The major decomposition event occurred between 300 °C and 400 °C, with a weight loss of

Table 1 Optimization data for synthesizing 1,2,4-triazolidine-3-thiones

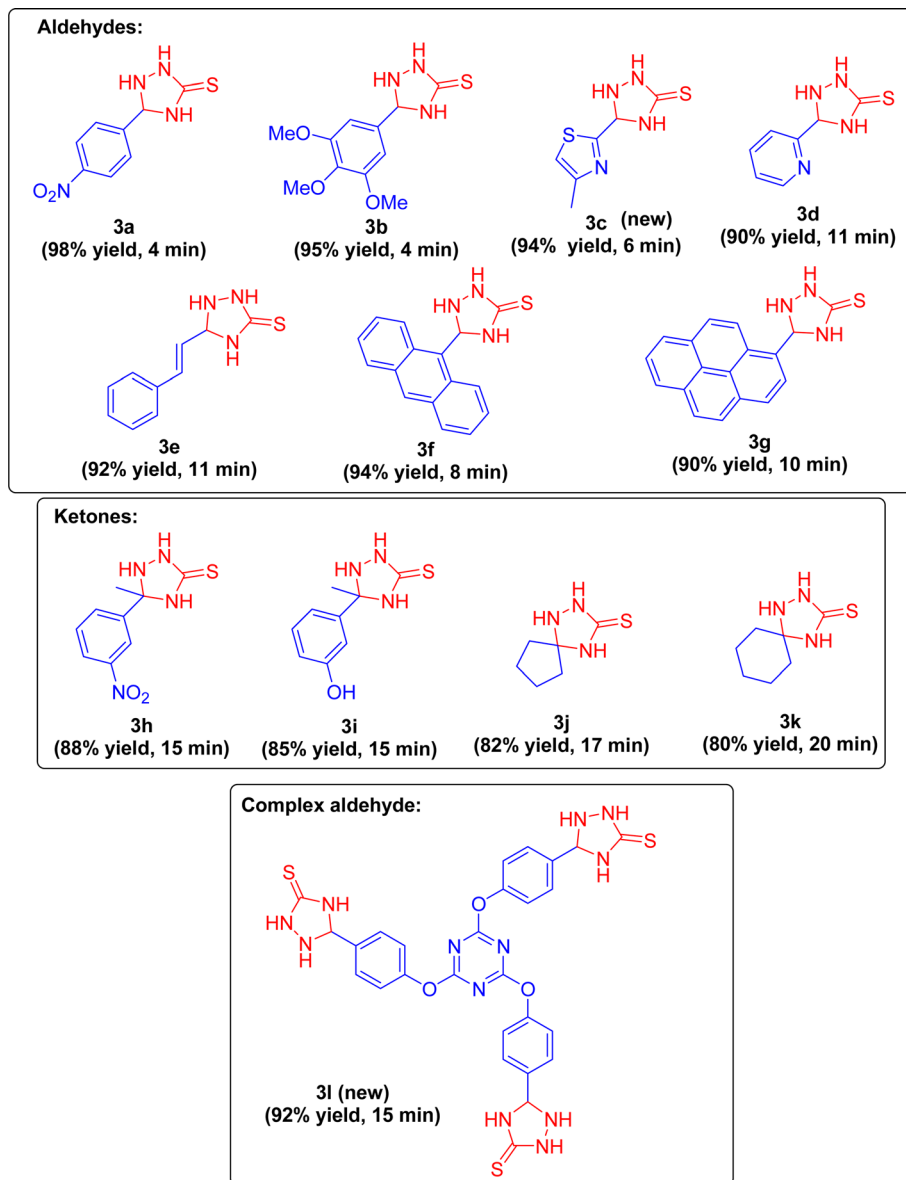| S. No.	Catalyst loading	Solvent	Temperature	Yield	Time (min)
1	No catalyst	H$_2$O	RT	42%	120
2	5 mg	H$_2$O	RT	60%	30
3	10 mg	H$_2$O	RT	68%	30
4	15 mg	H$_2$O	RT	80%	20
5	20 mg	H$_2$O	RT	90%	10
6	25 mg	H$_2$O	RT	89%	10
7	20 mg	EtOH	RT	92%	10
8	20 mg	MeOH	RT	90%	20
9	20 mg	Dioxane	RT	82%	25
10	20 mg	THF	RT	85%	25
11	20 mg	H$_2$O : EtOH (1 : 1)	RT	98%	6
12	20 mg	H$_2$O : EtOH (1 : 2)	RT	98%	4
13	20 mg	H$_2$O : EtOH (1 : 2)	50 °C	96%	5
14	20 mg	H$_2$O : EtOH (1 : 2)	80 °C	96%	5

Fig. 6 Synthesized derivatives of T-3-Ts.

approximately 48.4%, corresponding to the breakdown of the organic framework. Beyond 400 °C, the TGA curve stabilized, indicating the formation of a thermally stable carbonaceous residue. These results suggest that the COF is thermally stable up to 300 °C, after which significant degradation occurs, limiting its application in high-temperature environments.
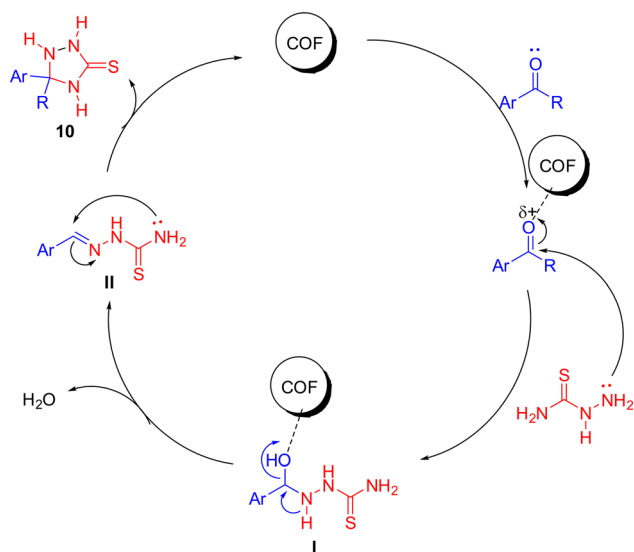
DTA

Differential Thermal Analysis (DTA) was performed alongside TGA to identify the thermal events associated with the COF's decomposition. The DTA curve (Fig. 5b) displayed a slight endothermic peak at around 100 °C, corresponding to the removal of adsorbed water. A broad exothermic peak between 300 °C and 400 °C was observed, associated with the exothermic decomposition of the organic framework, consistent with the

major weight loss seen in TGA. The stabilization of the DTA curve beyond 400 °C aligns with the TGA data, confirming that the remaining residue is thermally stable and does not undergo further significant thermal events.

The comprehensive characterization of the synthesized COF reveals a material with promising structural, morphological, and thermal properties. The FTIR and XPS analyses confirmed the successful formation of the desired chemical linkages, while XRD showed a well-ordered crystalline structure. SEM and TEM analyses highlighted the uniformity in particle size and morphology, which is essential for reproducibility. BET analysis indicated moderate surface area and mesoporosity, which are advantageous for catalytic applications. Thermal analysis *via* TGA and DTA demonstrated that the COF is stable up to 300 °C, after which it decomposes, limiting its use in higher-temperature environments. These findings suggest that the

Scheme 4 Proposed reaction mechanism for synthesis of T-3-Ts derivatives.

synthesized COF could be a suitable candidate for applications requiring moderate thermal stability and well-defined structural properties.

After the characterization of the prepared COF, their catalytic application was explored in organic synthesis for the synthesis of T-3-Ts through the reaction of TSC with various ketones and aldehydes. A set of experiments were systematically conducted on the reaction of 4-nitrobenzaldehyde and TSC to establish the best reaction conditions, including catalyst loading, solvent choice, and temperature (Scheme 2). The findings are outlined in Table 1.

This study explores the optimization of catalyst loading and solvent choice to enhance yield and efficiency in a chemical reaction. The results revealed a strong correlation between catalyst loading and yield, with an increase from 0 mg to 25 mg elevating the yield from 42% to 89% and reducing the reaction time from 120 minutes to 10 minutes (Table 1, entries 1–6). Notably, the most significant improvement occurred between 5 mg and 15 mg, where yield increased from 60% to 80%. When evaluating solvent effects, a 1 : 2 mixture of water and ethanol outperformed other solvents, achieving a yield of 98% in just 4 minutes, compared to 90% in 10 minutes with water alone. Other solvents, such as methanol, dioxane, and THF, yielded between 82% and 92% but require longer reaction times (Table 1, entries 7–12). The temperature variations from room temperature to 50 °

C or 80 °C show minimal impact on yield or reaction time with the optimal solvent and catalyst loading, maintaining a yield of 96% and a reaction time of 5 minutes (Table 1, entries 13 and 14). Ultimately, the optimal conditions identified are 20 mg of catalyst, a 1 : 2 water: ethanol solvent ratio, and room temperature, resulting in a yield of 98% in 4 minutes, indicating a well-balanced approach to maximize the reaction efficiency.

To evaluate the protocol's effectiveness and explore the range of the two-component cyclocondensation reaction involving aryl and heteroaryl aldehydes with TCS, a variety of structurally different aldehydes including both aromatic and hetero aromatic species were tested (Scheme 3). These aldehydes reacted efficiently with TCS, yielding the corresponding T-3-Ts in very high to excellent yields. Notably, the newly synthesized TRIPOD smoothly converted with TCS, producing the corresponding **3l** (novel) in excellent yields (92%). Further investigation into the scope involved use of acetophenones and cyclic ketones with TCS under optimized experimental parameters, which also resulted in the desired T-3-Ts in remarkable yields Fig. 6.

Based on the review of existing literature,[43] a plausible mechanism has been proposed (Scheme 4). The reactants were adsorbed onto the surface of the COF and the mechanism proceeds through the following steps.

1. Activation of the carbonyl compound by the COF. ● The nitrogen and oxygen atoms in the COF structure, as confirmed by XPS, interacted with the carbonyl group (C=O) of aldehydes or ketones, leading to its activation by polarization. This step weakened the carbonyl bond, making the carbonyl carbon more electrophilic.

2. Nucleophilic attack by thiosemicarbazide. ● Once the carbonyl compound was activated on the COF surface, thiosemicarbazide (TSC) acted as a nucleophile. The –NH$_2$ group of TSC attacked the electrophilic carbonyl carbon, forming an intermediate hydrazone structure (I).

● This reaction led to the formation of a C=N bond between the TSC and the carbonyl compound, which aligned with the hydrazone linkages present in the COF structure. The porous and moderate surface area of the COF, as suggested by BET analysis, facilitated this adsorption and reaction.

3. Cyclization step (triazolidine formation). ● After the hydrazone intermediate was formed, intramolecular cyclization occurred. The –NH group in thiosemicarbazide attacked the C=N bond, leading to the formation of the 1,2,4-triazolidine ring.

● During this cyclization process, a proton transfer helped in stabilizing the ring structure, forming a five-membered heterocyclic system.

Table 2 Comparative study of the present method with previous methods for the synthesis of T-3-Ts derivatives

S. No.	Catalyst	Reaction conditions	Yield	Time	Reference
1	—	25% EtOH; 80 °C	86–95%	7–15 min	44
2	3% Sm/FAp	H$_2$O; R.T.	90–97%	15–30 min	45
3	VB$_1$	H$_2$O; R.T.	65–94%	12–180 min	43
4	CoCr$_2$O$_4$ NPs	H$_2$O : EtOH (1 : 1); R.T.	96–99%	2.5–5 min	46
5	Meglumine	H$_2$O; R.T.	85–92%	5–8 min	47
6	Hydrazone-based COF	H$_2$O : EtOH (1 : 2); R.T.	80–98%	4–20 min	Present work

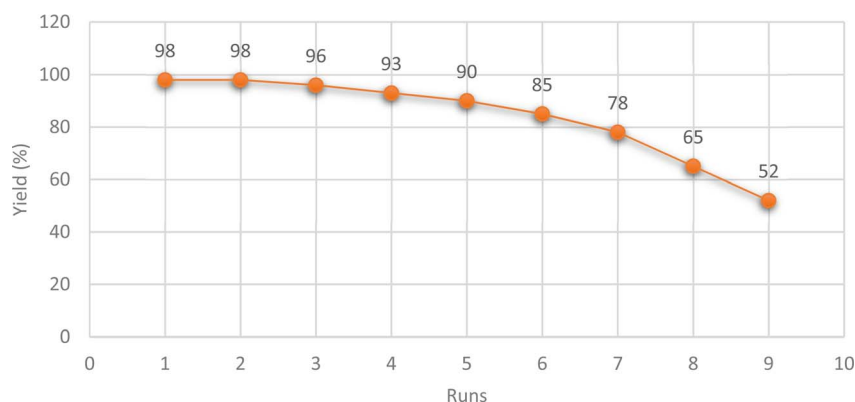## Reusability study of COF

Fig. 7 Recyclability study of the COF as a catalyst for synthesis of T-3-Ts scaffolds.

• The COF served as a heterogeneous catalyst throughout the reaction, facilitating the adsorption, activation, and cyclization steps.

Role of the COF as a catalyst

• The mesoporous structure of the COF, as indicated by BET surface area and pore size distribution, provided a high surface area for reactant molecules to adsorb, allowing the efficient interaction between the carbonyl compounds and thiosemicarbazide.

• The nitrogen- and oxygen-rich sites and hydrazone linkages in the COF framework, confirmed by FTIR and XPS, contributed to the activation of carbonyl groups, enhancing the electrophilicity of the substrate and promoting nucleophilic attack.

• The heterogeneous nature of the COF catalyst allowed for the easy separation of the catalyst from the reaction mixture, with no contamination of the final product.

Furthermore, the reusability study of the catalyst was performed on the model reaction. After the completion of the reaction, more ethanol was mixed with the reaction mixture to separate the product, and the COF was separated through simple filtration. Then the catalyst was again washed with ethanol and reused for the next run. The yield was calculated in 4 minutes of reaction time. In six reusability tests, no appreciable change in the yield was seen; afterwards the yield was significantly decreased but the COF was reused up to eight runs with significant catalytic activity (Fig. 7). Furthermore, a comparative study of the present method for the synthesis of T-3-Ts compounds was performed with previous methods as summarized in Table 2. The results illustrated the effectiveness of the developed protocol for the synthesis of T-3-Ts scaffolds and efficient catalytic activity of the prepared COF as shown in Fig. 7.

Conclusion

In this study, we have successfully synthesized a novel hydrazone-linked covalent organic framework (COF) using synthesized TRIPOD and DHTH. The synthesis process, which involved the ultrasonic treatment of TRIPOD and DHTH in a blend of 1,4-dioxane and aqueous acetic acid, yielded pale-yellow COF powders, insoluble in common organic solvents. The characterization through FT-IR, PXRD, SEM, TEM, XPS, BET, TGA, and DTA confirmed the successful formation and crystalline structure of the stable COF, with a consistent spherical morphology and a crystallite size of 23.24 nm. The COF showed a surface area of 2.78 m^2 g^{-1} and mesoporous characteristics, essential for catalytic activities. Moreover, the synthesized COF showed thermal stability up to 300 °C. This stability and porosity played a key role in its catalytic performance in the production of 1,2,4-triazolidine-3-thiones from thiosemicarbazide and various ketones and aldehydes. The optimization of reaction conditions revealed that a catalyst loading of 20 mg, a 1 : 2 water : ethanol solvent ratio, and room temperature were ideal, achieving high to excellent yields (80–98%) of products in a very low reaction time (4–20 min). The reusability tests demonstrated that the COF exhibited consistent catalytic activity across eight cycles of reuse without substantial degradation. Overall, this research highlights the potential of hydrazone-linked COFs in catalysis, providing a new avenue for their application in synthetic chemistry. The straightforward synthesis, combined with excellent catalytic performance and reusability, underscores the viability of these COFs for future catalytic processes.

Data availability

The data related to the manuscript are available in the ESI file.†

Conflicts of interest

The authors confirmed that this article has no conflict of interest.

Acknowledgements

References

1 S.-Y. Ding and W. Wang, *Chem. Soc. Rev.*, 2013, **42**, 548–568.

2 N. Huang, P. Wang and D. Jiang, *Nat. Rev. Mater.*, 2016, **1**, 16068.

3 M. S. Lohse and T. Bein, *Adv. Funct. Mater.*, 2018, **28**, 1705553.

4 J. Xiao, J. Chen, J. Liu, H. Ihara and H. Qiu, *Green Energy Environ.*, 2023, **8**, 1596–1618.

5 J. Hu, Z. Huang and Y. Liu, *Angew. Chem., Int. Ed.*, 2023, **62**, e202306999.

6 P. T. Parvatkar, S. Kandambeth, A. C. Shaikh, I. Nadinov, J. Yin, V. S. Kale, G. Healing, A.-H. Emwas, O. Shekhah, H. N. Alshareef, O. F. Mohammed and M. Eddaoudi, *J. Am. Chem. Soc.*, 2023, **145**, 5074–5082.

7 S. Liu, Q. Su, W. Qi, K. Luo, X. Sun, H. Ren and Q. Wu, *Catal. Sci. Technol.*, 2022, **12**, 2837–2845.

8 M. Tian, S. Liu, X. Bu, J. Yu and X. Yang, *Chem.–Eur. J.*, 2020, **26**, 369–373.

9 A. Jiménez-Almarza, A. López-Magano, L. Marzo, S. Cabrera, R. Mas-Ballesté and J. Alemán, *ChemCatChem*, 2019, **11**, 4916–4922.

10 P. Pachfule, A. Acharjya, J. Roeser, T. Langenhahn, M. Schwarze, R. Schomäcker, A. Thomas and J. Schmidt, *J. Am. Chem. Soc.*, 2018, **140**, 1423–1427.

11 K. Asokan, M. K. Patil, S. P. Mukherjee, S. B. Sukumaran and T. Nandakumar, *Chem.–Asian J.*, 2022, **17**, e202201012.

12 Q. N. Tran, H. J. Lee and N. Tran, *Polymers*, 2023, **15**, 1279.

13 X. Zhang, G. Li, D. Wu, B. Zhang, N. Hu, H. Wang, J. Liu and Y. Wu, *Biosens. Bioelectron.*, 2019, **145**, 111699.

14 R. Davis, R. A. Urbanowski and A. K. Gaharwar, *Curr. Opin. Biomed. Eng.*, 2021, **20**, 100319.

15 A. Murali, G. Lokhande, K. A. Deo, A. Brokesh and A. K. Gaharwar, *Mater. Today*, 2021, **50**, 276–302.

16 H. H. Hegazy, S. S. Sana, T. Ramachandran, Y. A. Kumar, D. K. Kulurumotlakatla, H. S. M. Abd-Rabboh and S. C. Kim, *J. Energy Storage*, 2023, **74**, 109405.

17 S.-X. Gan, C. Jia, Q.-Y. Qi and X. Zhao, *Chem. Sci.*, 2022, **13**, 1009–1015.

18 H. Hu, Q. Yan, R. Ge and Y. Gao, *Chin. J. Catal.*, 2018, **39**, 1167–1179.

19 Z. Alsudairy, N. Brown, A. Campbell, A. Ambus, B. Brown, K. Smith-Petty and X. Li, *Mater. Chem. Front.*, 2023, **7**, 3298–3331.

20 D. Ma, Y. Wang, A. Liu, S. Li, C. Lu and C. Chen, *Adv. Energy Mater.*, 2018, **8**, 1702170.

21 S. Pasricha, A. Chaudhary and A. Srivastava, *ChemistrySelect*, 2022, **7**, e202200576.

22 Y. Zhi, Z. Wang, H.-L. Zhang and Q. Zhang, *Small*, 2020, **16**, 2001070.

23 S. S. A. Shah, M. S. Javed, T. Najam, M. A. Nazir, A. ur Rehman, A. Rauf, M. Sohail, F. Verpoort and S.-J. Bao, *Mater. Today*, 2023, **67**, 229–255.

24 J. Guo and D. Jiang, *ACS Cent. Sci.*, 2020, **6**, 869–879.

25 N. Khaleghi, M. Esmkhani, M. Noori, N. Dastyafteh, M. K. Ghomi, M. Mahdavi, M. H. Sayahi and S. Javanshir, *Nanoscale Adv.*, 2024, **6**, 2337–2349.

26 R. Bakhshali-Dehkordi, M. A. Ghasemzadeh and J. Safaei-Ghomi, *J. Mol. Struct.*, 2020, **1206**, 127698.

27 M. A. Ghasemzadeh, B. Mirhosseini-Eshkevari and M. H. Abdollahi-Basir, *Comb. Chem. High Throughput Screening*, 2016, **19**, 592–601.

28 R. H. Althomali, E. A. Musad Saleh, R. H. Mohammed Ali, I. I. Mamadoliev, M. F. Ramadan, A. T. Kareem, S. Aggarwal and S. K. Hadrawi, *Nanoscale Adv.*, 2023, **5**, 6177–6193.

29 B. Mirhosseini-Eshkevari, M. A. Ghasemzadeh and M. Esnaashari, *Appl. Organomet. Chem.*, 2019, **33**, e5027.

30 J. Safaei-Ghomi, M. A. Ghasemzadeh and A. Kakavand-Qalenoei, *J. Saudi Chem. Soc.*, 2016, **20**, 502–509.

31 P. G. Mahajan, N. C. Dige, B. D. Vanjare, H. Raza, M. Hassan, S.-Y. Seo, C.-H. Kim and K. H. Lee, *Mol. Diversity*, 2020, **24**, 1185–1203.

32 H. Adibi, R. Abiri, S. Mallakpour, M. A. Zolfigol and M. B. Majnooni, *J. Rep. Pharm. Sci.*, 2012, 1.

33 W. M. Huggins, B. M. Minrovic, B. W. Corey, A. C. Jacobs, R. J. Melander, R. D. Sommer, D. V. Zurawski and C. Melander, *ACS Med. Chem. Lett.*, 2017, **8**, 27–31.

34 N. U. Hebbar, P. S. Hebbar, P. P. Rathode, B. Negalura, A. Hiremath, P. Gudimani, L. A. Shastri, S. K. Praveen Kumar, A. J. Kadapure and S. Joshi, *J. Mol. Struct.*, 2023, **1280**, 135003.

35 V. Kanagarajan, J. Thanusu and M. Gopalakrishnan, *Med. Chem. Res.*, 2012, **21**, 3965–3972.

36 F. Shaikh, S. L. Shastri, N. S. Naik, R. Kulkarni, J. M. Madar, L. A. Shastri, S. D. Joshi and V. Sunagar, *ChemistrySelect*, 2019, **4**, 105–115.

37 H. Adibi, L. Hosseinzadeh, M. Mahdian, A. Foroumadi, M. A. Zolfigol and S. Mallakpour, *J. Rep. Pharm. Sci.*, 2013, 2.

38 J. A. Mikroyannidis, S. S. Sharma, Y. K. Vijay and G. D. Sharma, *ACS Appl. Mater. Interfaces*, 2010, **2**, 270–278.

39 L. R. Ahmed, A. F. M. El-Mahdy, C.-T. Pan and S.-W. Kuo, *Mater. Adv.*, 2021, **2**, 4617–4629.

40 S. Haldar, K. Roy, S. Nandi, D. Chakraborty, D. Puthusseri, Y. Gawli, S. Ogale and R. Vaidhyanathan, *Adv. Energy Mater.*, 2018, **8**, 1702170.

41 H. M. El-Kaderi, J. R. Hunt, J. L. Mendoza-Cortés, A. P. Côté, R. E. Taylor, M. O'Keeffe and O. M. Yaghi, *Science*, 2007, **316**, 268–272.

42 S. Zeghdi, S. E. Laouini, H. A. Mohammed, A. Bouafia, M. L. Tedjani, M. M. S. Abdullah and T. Trzepieciński, *Materials*, 2024, **17**, 2358.

43 P. J. Patil, G. D. Salunke, M. B. Deshmukh, S. P. Hangirgekar, D. R. Chandam and S. A. Sankpal, *ChemistrySelect*, 2019, **4**, 13071–13078.

44 R. Ramesh and A. Lalitha, *ChemistrySelect*, 2016, **1**, 2085–2089.

45 S. N. Maddila, S. Maddila, K. K. Gangu, W. E. van Zyl and S. B. Jonnalagadda, *J. Fluorine Chem.*, 2017, **195**, 79–84.

46 S. Ghotekar, D. Sanap, K.-Y. A. Lin, H. Louis, D. Pore and R. Oza, *Res. Chem. Intermed.*, 2024, **50**, 49–68.

47 L. B. Masram, S. S. Salim, A. B. Barkule, Y. U. Gadkari and V. N. Telvekar, *J. Chem. Sci.*, 2022, **134**, 94.